

Superfragile Glassy Dynamics of a One-Component System with Isotropic Potential: Competition of Diffusion and Frustration

R. E. Ryltsev,¹ N. M. Chtchelkatchev,^{2,3,4} and V. N. Ryzhov^{2,3}

¹*Institute of Metallurgy, Ural Division of Russian Academy of Sciences, Yekaterinburg 620017, Russia*

²*Institute for High Pressure Physics, Russian Academy of Sciences, 142190 Troitsk, Russia*

³*Moscow Institute of Physics and Technology, 141700 Moscow, Russia*

⁴*L. D. Landau Institute for Theoretical Physics, Russian Academy of Sciences, 117940 Moscow, Russia*

(Received 10 October 2012; published 7 January 2013)

We investigate glassy dynamical properties of one-component three-dimensional system of particles interacting via pair repulsive potential by the molecular dynamic simulation in the wide region of densities. The glass state is superfragile and it has high glass-forming ability. The glass transition temperature T_g has a pronounced minimum at densities where the frustration is maximal.

DOI: [10.1103/PhysRevLett.110.025701](https://doi.org/10.1103/PhysRevLett.110.025701)

PACS numbers: 64.70.Q-, 61.20.Gy, 61.20.Ne

The ubiquitous glass formation and jamming still puzzle physicists [1,2]. The microscopic mechanism of the drastic slowing down of the structural relaxation of a liquid upon cooling is one of the central issues of the physics of the liquid-glass transition. The question “why some liquids form a glass easily but others do not” is still the matter of debates.

There is a paradigm that one-component liquid with isotropic potential typically spontaneously crystallizes being supercooled in (quasi)equilibrium conditions [3–6]. It is a formidable challenge to avoid, e.g., spontaneous crystallization in quasiequilibrium cooling of the one-component Lennard-Jones liquid. Yet, it was discovered not long ago that there are some exceptions from the paradigm. The common fitch of these exceptions is the pronounced attractive well of the pair potential, see, e.g., Refs. [7,8]. Here, we show using the molecular dynamics simulation (MD) that the one-component simple liquid with *pure repulsive potential* shows glassy behavior in quasiequilibrium cooling.

Frustration, when one cannot minimize the energy of the system by merely minimizing all local interactions, is one of the basic factors that stipulates the glass-forming ability [1,9]. For example, it can be related with the long-range alternating interactions (e.g., in spin glasses [10]) or with geometrical reasons [11]. The potential used in Refs. [7,8] was optimized to produce icosahedral local order and so, geometrical frustration. Our potential has the soft step and the simple liquid with this interaction has two characteristic scales. The competition between these scales makes the system effectively quasibinary [12]. And this is the origin of frustration in our system. Intuitively increasing frustration, one should favor the formation of the glass. Here, we show that on the contrary, the glass transition temperature T_g may have minimum at parameters where the frustration is maximal.

The second important concept of glassy physics is fragility. According to Angell-classification [2,13], the

glass-forming liquids effectively divide into two classes: “strong” and “fragile”, where the viscosity of the liquid shows either nearly Arrhenius behavior with temperature or a much faster one. We found the fragility index and concluded that our system is superfragile (its fragility index exceeds that of the “Decalin”—one the most fragile liquids [14]), see Fig. 1.

We use the pair potential model of “collapsing soft spheres” [12,15,16]:

$$U(r) = \varepsilon \left(\frac{\sigma}{r} \right)^n + \varepsilon n_F [2k_0(r - \sigma_1)], \quad (1)$$

where $n_F(x) = 1/[1 + \exp(x)]$, ε is the unit of energy, σ and σ_1 are “hard”-core and “soft”-core diameters. This kind of potentials, Eq. (1), is successfully used for simulation of water-like anomalies, liquid-liquid phase transitions, and glass formation [12,15–20]. The graph of

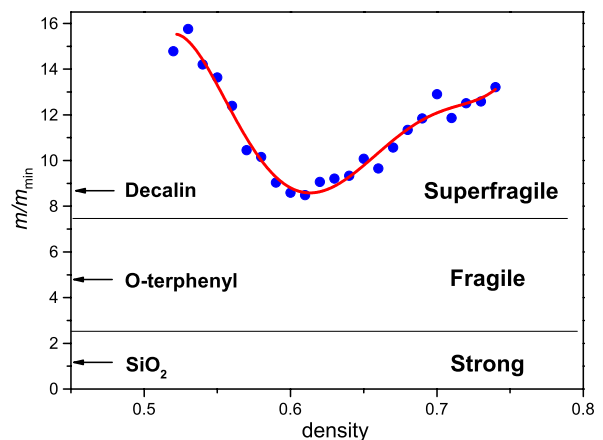


FIG. 1 (color online). Relative fragility of our system as a function of density. For comparison, we show the fragility of the typical glass-formers. Our system in the glass regime appears to be extremely fragile. It seems that it is in the short list of the most fragile glassy systems.

the potential, we discuss in the Supplemental Material [21] and in Fig. 5.

In the remainder of this Letter, we use the dimensionless quantities: $\tilde{\mathbf{r}} \equiv \mathbf{r}/\sigma$, $\tilde{U} = U/\varepsilon$, temperature $\tilde{T} = T/\varepsilon$, density $\tilde{\rho} \equiv N\sigma^3/V$, and time $\tilde{t} = t/[\sigma\sqrt{m/\varepsilon}]$, where m and V are the molecular mass and system volume, correspondingly. As we will only use these reduced variables, we omit the tildes. So, we take here $n = 14$, $k_0 = 10$, and $\sigma_1 = 1.35$. These parameter values reveal complex system behavior such as phase diagram with polymorphous transitions and disordered gap, see Fig. 2, and water-like anomalies [12,15,16].

For MD simulations, we have used the system of $N = 5000$ particles that were simulated under periodic boundary conditions in a Nose-Hoover NVT ensemble. We have checked that $N = 5000$ is an enough amount of particles to eliminate the finite size effects that agrees with Ref. [21]. The MD time step was $\delta t = 0.01$. It is nearly the maximum possible time step that satisfies the energy conservation condition. The system was studied in the density region of $\rho \in (0.35-0.75)$. At all densities of this region, the system was cooled in a stepwise manner from high temperature state and completely equilibrated at each step until convergence of time dependence of mean square displacement (up to 5×10^7 time steps). The time dependencies of temperature, pressure, and configuration energy were additionally analyzed to control equilibration. Data were, subsequently, collected during the time t_{samp} that was chosen to be large enough for correct calculation of diffusion coefficients by the Einstein relation. So this time was approximately equal to $t_{\text{samp}} \sim 3\tau$, where τ is the time necessary to reach diffusive regime after ballistic and plateau ones. For more details, see Supplemental Material [21].

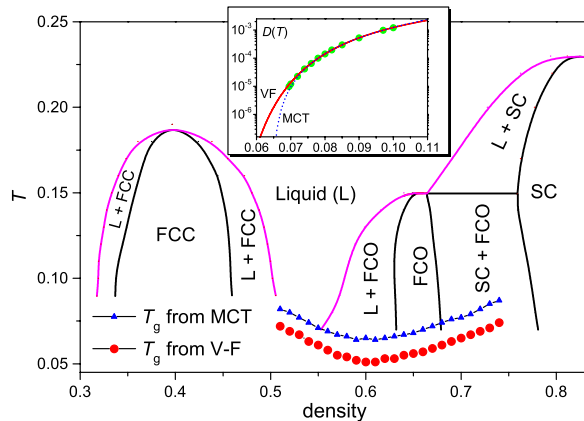


FIG. 2 (color online). We show the glass transition temperature on the sketch of the phase diagram obtained in Ref. [12]. The red circles and blue triangles correspond to T_g extracted from $D(T)$ using the Vogel-Fulcher formula (VF) [29] and the power law from mode-coupling theory (MCT) [31], correspondingly. In the inset, we show the accuracy of $D(T)$ approximation by VF and MCT for $\rho = 0.6$. The circles show the result of MD simulations.

Avoiding spontaneous crystallization during equilibration process is the principal difficulty of MD simulations of glassy dynamics of liquids. For model glass-forming systems, this problem is usually solved by either using nonisotropic potentials [5,22], or considering multi-component systems [23,24], using nonequilibrium cooling [18,25]. For collapsing soft spheres system, it is possible to avoid crystallization in the one-component system with isotropic potential due to the quasibinary behavior that develops itself in certain density interval. In our case, this range is $\rho \in (0.51-0.74)$. In the inset in Fig. 3(b), we show the splitting of the first peak in the radial distribution functions (RDF) that illustrates the quasibinary behavior of our system in hand. Outside this interval, it is hardly possible to study the glassy dynamics because the system spontaneously crystallizes, whereupon, supercooling below the melting line. Conversely, inside the region mentioned, one can equilibrate supercooled liquid without crystallization down to temperatures at which relaxation time becomes too large for simulation. In our case, these minimal temperatures were chosen so that diffusion coefficients were on the order of 10^{-5} . At those temperatures, the total calculation time required for equilibration and data collecting is $\sim 3 \times 10^7$ MD steps (three days of calculation on 32 processors in parallel).

In order to control stability of glassy state, we performed calculations at lower temperatures also (down to T_g). At those temperatures, the system cannot be equilibrated completely because of large relaxation times and so we did not use these data for T_g calculations. But what we have observed is the absence of any crystallization up to 10^8 MD steps and so, we conclude that the glass state is stable (at least at simulation time scales).

To acquire information about the glass state, we focus on the temperature range $T \geq T_g$ where the “glass-forming fluctuations” [26] slow down the system dynamics with temperature decreasing. The conventional correlation function tools have been used: the mean square displacement $\Delta r^2(t)$ and the intermediate scattering function $F_s(q, t)$. The time dependencies of these functions for $\rho = 0.6$ and different temperatures are shown in Fig. 4. One can see the typical picture glass-formers demonstrate at low temperatures [27]. Namely, the “plateau” reflecting the cage effect (when the particle is trapped in the “cage” of the nearest neighbors) appears on $\Delta r^2(t)$ and $F_s(q, t)$ at sufficiently low temperatures that indicates the onset of the glassy regime in system dynamics. Meanwhile, the system remains in a disordered state as can be seen from radial distribution functions, see inset of Fig. 3(b). We note the splitting of the first and second peaks of the radial distribution function [Fig. 3(b)]. The splitting of the first peak reflects the quasibinary of the system caused by the form of the potential (see discussion below); while the splitting of the second peak is apparently the (system independent) attribute of the glassy state [7,18,28].

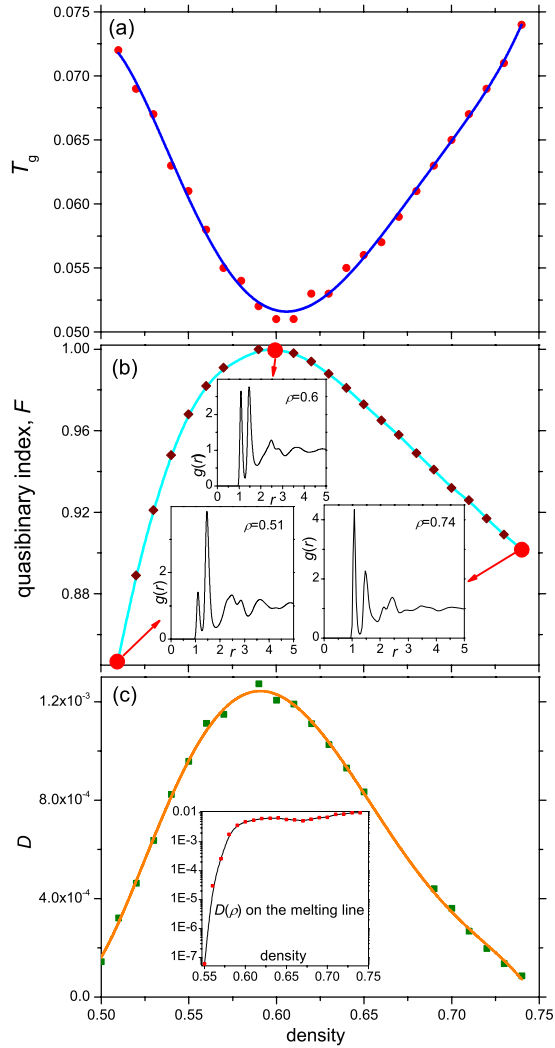


FIG. 3 (color online). (a) $T_g(\rho)$ (using VF). (b) Quasibinary index, F , for $T = 0.1$ and the range of densities where the glassy dynamics was detected. Comparing the $F(\rho)$ with $T_g(\rho)$, we see that these dependencies are opposite to one another: the bigger F , the smaller T_g and the maximum of the former curve is located at the same density as the minimum of the later one. The inset shows the radial distribution function $g(r)$. It has two clear peaks at $r = d$, $r = \sigma$ that proves the quasibinary behavior of the system. (c) The diffusion coefficient $D(\rho)$ for $T = 0.1$.

In order to estimate the glass transition temperature, we calculated diffusion coefficient D at each of the temperatures and densities investigated. The temperature dependencies $D(T)$ were approximated by both the Vogel-Fulcher formula (VF) [29,30]

$$D = D_0^{(\text{VF})} \exp\left(-\frac{A}{T - T_0^{(\text{VF})}}\right) \quad (2)$$

and the power law from mode-coupling theory (MCT) [30,31]

$$D = D_0^{(\text{MC})} (T - T_0^{(\text{MC})})^\gamma. \quad (3)$$

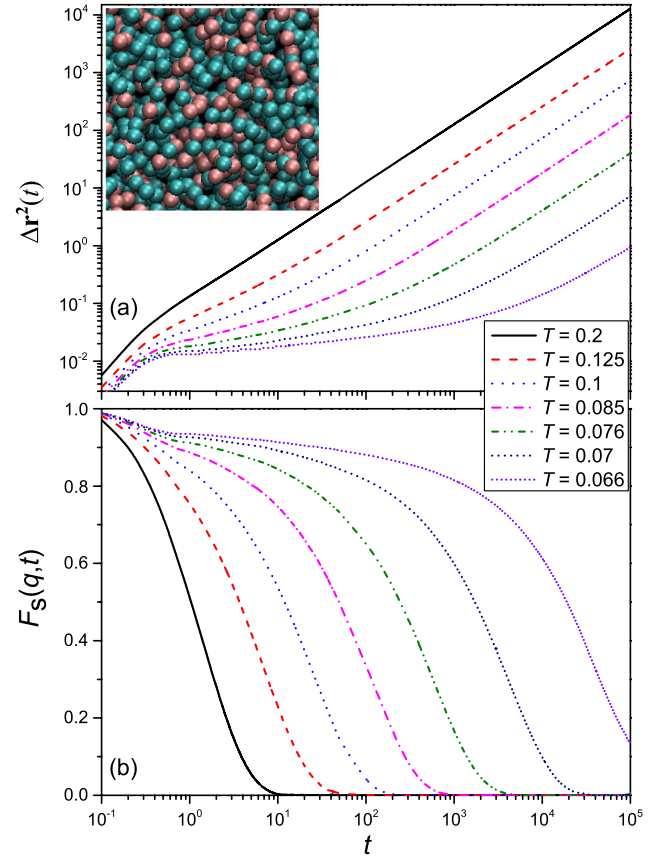


FIG. 4 (color online). (a) Mean-square displacement and (b) intermediate scattering function for the density $\rho = 0.6$. Inset shows the snapshot of the typical distribution of particles for $T = 0.1$ and $\rho = 0.6$. We mark by red or light gray (blue or dark gray) color particles that have a neighbor at a distance of the order of the first (second) maximum in RDF (hard-core and soft-core diameters).

The parameters $D_0^{(\text{VF})}$, A , $T_0^{(\text{VF})}$, $D_0^{(\text{MC})}$, $T_0^{(\text{MC})}$, and γ were obtained using the method of nonlinear least squares. Since the expressions of Eqs. (2) and (3) are correct only in the vicinity of a glass transition temperature, the temperature interval $T \in (T_{\min}, T_{\max})$ for least squares approximation was chosen so that $D(T_{\min}) \approx 10^{-5}$, $D(T_{\max}) \approx 10^{-3}$ that approximately corresponds $T/T_g \in (1.15, 1.6)$. The typical temperature dependence $D(T)$ of diffusion coefficient obtained from simulations and its VF and MCT approximations are shown in the inset of Fig. 2. One can see that both formulas provide good fitting of simulation data.

Having the parameters of Eqs. (2) and (3), one can get the glass transition temperature. According to generally accepted definition, glass transition occurs at $D_0/D = 10^n$, where $13 \lesssim n \lesssim 17$. Using Eqs. (2) and (3), we obtain

$$T_g^{(\text{VF})} = T_0^{(\text{VF})} + \frac{A \log_{10} e}{n}, \quad (4)$$

$$T_g^{(\text{MC})} = T_0^{(\text{MC})} + 10^{-n/\gamma}. \quad (5)$$

The graph of $T_g(\rho)$ is shown in Fig. 2 on the phase diagram (previously obtained in Ref. [12]). It follows that $T_g(\rho)$ dependencies obtained using VF and MCT approaches are in good agreement with each other. Particularly, both curves are located under the melting line and have a minima in the vicinity of density $\rho = 0.6$.

We calculate the fragility index m showing the deviation of $D(T)$ from Arrhenius law and allowing us to identify the type of glass-forming system according to strong-fragile classification. Starting with the definition of fragility in the form [32–35]

$$m = \left. \frac{\partial \log_{10}(D_0/D)}{\partial (T_g/T)} \right|_{T=T_g} \quad (6)$$

and using Eqs. (2) and (4), we get

$$m = n \left(\frac{T_0^{(\text{VF})}}{A} n \ln 10 + 1 \right). \quad (7)$$

The Eq. (7) particularly shows that the fragility index has minimal value $m_{\min} = n$ corresponding to the limit $T_0^{(\text{VF})}/A \rightarrow 0$ that turns Eq. (2) into Arrhenius law. Figure 1 shows the density dependence of the reduced fragility, m/m_{\min} , of our system in comparison to several glass-formers. One can see that the dynamics of our system is extremely fragile since the mean value of its fragility exceeds the one for decalin—one of the most fragile systems [14]. Note that $m(\rho)$ is nonmonotonic and reveals clear minimum at $\rho = 0.6$ as well as for $T_g(\rho)$, see Fig. 2. Recently, it was shown that the increase of the interaction softness can lead to the increase of the fragility [34,35]. The “softness” of our pair potential is large at r , corresponding to the peaks of the radial distribution function, see Fig. 5. Away from $\rho^* = 0.6$, one of the RDF peaks dominates, see inset in Fig. 3(b), that effectively makes softer the effective interparticle interaction and helps to interpret the nonmonotonic behavior of $m(\rho)$.

Advances over the last decade have linked non-Arrhenius behavior of fragile glass-formers with the presence of locally heterogeneous dynamics: i.e., the presence of distinct (if transient) slow and fast regions within the material [2,36]. The quasibinary character of our particle

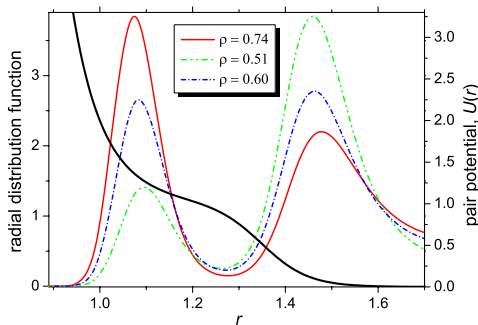


FIG. 5 (color online). The pair potential $U(r)$ and the splitted first peak of the radial distribution functions.

system allows us to make the selection among the particles: we mark by red (blue) color particles that have a neighbor at a distance of the order of the first (second) maximum in RDF (hard-core and soft-core diameters), see Fig. 5. The snapshot of the spatial particle distribution over the simulation volume (see inset in Fig. 4 and 2 in the Supplemental Material [21]) shows the high degree of the heterogeneity in our system that favors the existence of the locally heterogeneous dynamics within the system because of different free volumes (and so diffusion coefficients) of particles with different effective radii.

It has been mentioned above that the system demonstrates quasibinary behavior due to the repulsive shoulder of the pair potential, see inset in Fig. 3(b). It reflects the competition between hard-core and soft-core scales and, as a result, the frustration in the system. As the quasibinary index, we choose

$$F = \frac{2\rho_1\rho_2}{\rho_1^2 + \rho_2^2}, \quad (8)$$

where $\rho_1 = \rho \int_0^{r_1} r^2 g(r) dr / \int_0^{r_1} r^2 dr$ and $\rho_2 = \rho \int_{r_1}^{r_2} r^2 g(r) dr / \int_{r_1}^{r_2} r^2 dr$. Here, r_1 and r_2 are minima of the first and the second RDF peaks. So ρ_1 and ρ_2 are local densities in the vicinity of the peaks and F is their inverse symmetrized ratio.

The origin of the frustration in our system is the same as for binary soft sphere-like systems where the frustration is due to the large, local rearrangement of atoms required for the formation of a crystal from a fluid or glassy configuration [37]. This situation is caused by the presence of a second component and so, the frustration of such type increases with increasing concentration. Thus, the quasibinary index F can serve as frustration measure in our system. It is clear that if the value $F \approx 0$ corresponds to the situation, then only one of the scales dominates and so there is no frustration in the system. On the contrary, if $F \approx 1$, the competition is between hard-core and soft-core scales and so the frustrations are maximal. It should be noted that F depends on temperature as well as on density. In order to study the influence of frustration on glass-forming ability of the system, we calculate the density dependence of the frustration index at sufficiently low temperatures. In Fig. 3(b), we show $F(\rho)$ at $T = 0.08$ (of the order of T_g for all of the densities investigated). It follows from Fig. 3 that $F(\rho)$ and $T_g(\rho)$ have opposite behavior: the bigger F , the smaller T_g , and the maximum of the former curve is located at the same density as the minimum of the later one.

At the density ρ^* where $T_g(\rho)$ has a minimum, the system has potentially a number of different lattice constants as we mentioned above. If we imagined the long-range order formation at ρ^* , then the crystal would be strongly distorted by defects due to the competition of the different lattice constants. This situation should favor the diffusion and frustration at the same time, see Fig. 3. T_g is determined both by the diffusion and by the frustration:

diffusion tries to decrease T_g while the frustration does the opposite. However, the diffusion defeats frustration in our system, so T_g has minimum at ρ^* .

Finally, we discuss the boundaries of the density domain, $\rho \in (0.35-0.75)$. Beyond these boundaries, the glass-forming ability quickly decreases. This one can judge from the quick rise of the diffusion coefficient, $D(\rho)$, at the melting line, see inset in Fig. 3(c), and the destruction of the quasibinary behavior, see inset in Fig. 3(b).

In conclusion, we show using the molecular dynamics simulations that the one-component simple liquid with pure repulsive potential shows glassy behavior in quasiequilibrium cooling. We explain the nonmonotonic density dependence of T_g , frustration, the diffusion coefficient, and fragility by the evolution of the quasibinary properties of our system. We observe that our system belongs to the short list of the most fragile systems. Our system can be used as the simple toy model for investigation of the quasibinary frustrated systems. In the search for (super) fragility in the one-component repulsive simple liquids, one should test them for quasibinary.

We thank V. Brazhkin, Yu. Fomin, G. Rusakov, E. E. Tareyeva, E. Tsiok, L. D. Son, and M. Vasin for helpful discussions. The work was supported by Russian Foundation for Basic Research (Grants No. 12-03-00757-a, No. 10-02-00882-a, No. 10-02-00694a, No. 10-02-00700, and No. 11-02-00-341a), Ural Division of Russian Academy of Sciences (Grant No. RCP-12-P3), and Presidium of Russian Academy of Sciences (Program 12-P-3-1013). We are grateful to supercomputer center of Ural Branch of Russian Academy of Sciences for the access to “Uran” cluster.

-
- [1] L. Berthier and G. Biroli, *Rev. Mod. Phys.* **83**, 587 (2011).
 [2] P. G. Debenedetti and F. H. Stillinger, *Nature (London)* **410**, 259 (2001).
 [3] K. Binder and W. Kob, *Glassy Materials and Disordered Solids. An Introduction to Their Statistical Mechanics* (World Scientific, Singapore, 2005).
 [4] W. Kob, *J. Phys. Condens. Matter* **11**, R85 (1999).
 [5] V. Molinero, S. Sastry, and C. A. Angell, *Phys. Rev. Lett.* **97**, 075701 (2006).
 [6] B. Bernu, Y. Hiwatari, and J. P. Hansen, *J. Phys. C* **18**, L371 (1985); B. Bernu, J. P. Hansen, Y. Hiwatari, and G. Pastore, *Phys. Rev. A* **36**, 4891 (1987).
 [7] M. Dzugutov, *Phys. Rev. A* **46**, R2984 (1992).
 [8] M. Elenius, T. Oettel, and M. Dzugutov, *J. Chem. Phys.* **133**, 174502 (2010).
 [9] H. Shintani and H. Tanaka, *Nat. Phys.* **2**, 200 (2006).
 [10] L. F. Cugliandolo, in *Slow Relaxations and Nonequilibrium Dynamics in Condensed Matter: Session LXXVII*, edited by J. L. Barrat, M. Feigelman, J. Kurchan, and J. Dalibard, (Springer, Berlin, 2003); *Spin Glasses and Random Fields*, edited by A. P. Young (World Scientific, Singapore, 1998).
 [11] G. Tarjus, S. A. Kivelson, Z. Nussinov, and P. Viot, *J. Phys. Condens. Matter* **17**, R1143 (2005).
 [12] Yu. D. Fomin, N. V. Gribova, V. N. Ryzhov, S. M. Stishov, and D. Frenkel, *J. Chem. Phys.* **129**, 064512 (2008).
 [13] C. A. Angell, *J. Non-Cryst. Solids* **102**, 205 (1988); C. A. Angell, *Science* **267**, 1924 (1995).
 [14] K. Duwuri and R. Richert, *J. Chem. Phys.* **117**, 4414 (2002).
 [15] N. V. Gribova, Yu. D. Fomin, D. Frenkel, and V. N. Ryzhov, *Phys. Rev. E* **79**, 051202 (2009).
 [16] Yu. D. Fomin, E. N. Tsiok, and V. N. Ryzhov, *J. Chem. Phys.* **134**, 044523 (2011); **135**, 234502 (2011).
 [17] G. Franzese, *J. Mol. Liq.* **136**, 267 (2007); P. Vilaseca and G. Franzese, *J. Non-Cryst. Solids* **357**, 419 (2011).
 [18] L. Xu, I. Ehrenberg, S. V. Buldyrev, and H. E. Stanley, *J. Phys. Condens. Matter* **18**, S2239 (2006); L. Xu, N. Giovambattista, S. V. Buldyrev, P. G. Debenedetti, and H. E. Stanley, *J. Chem. Phys.* **134**, 064507 (2011).
 [19] A. B. de Oliveira, P. A. Netz, Th. Colla, and M. C. Barbosa, *J. Chem. Phys.* **124**, 084505 (2006); **125**, 124503 (2006); **128**, 064901 (2008).
 [20] S. V. Buldyrev, G. Malescio, C. A. Angell, N. Giovambattista, S. Prestipino, F. Saija, H. E. Stanley, and L. Xu, *J. Phys. Condens. Matter* **21**, 504106 (2009).
 [21] See Supplemental Material at <http://link.aps.org/supplemental/10.1103/PhysRevLett.110.025701> for the detailed description of potential and simulations.
 [22] J. Horbach, W. Kob, K. Binder, and C. A. Angell, *Phys. Rev. E* **54**, R5897 (1996).
 [23] B. W. H. van Beest, G. J. Kramer, and R. A. van Santen, *Phys. Rev. Lett.* **64**, 1955 (1990).
 [24] T. A. Weber and F. H. Stillinger, *Phys. Rev. B* **31**, 1954 (1985).
 [25] W. Kob and H. C. Andersen, *Phys. Rev. E* **51**, 4626 (1995); **52**, 4134 (1995).
 [26] T. Mizuguchi and T. Odagaki, *Phys. Rev. E* **79**, 051501 (2009).
 [27] M. G. Vasin, N. M. Chetkatchev, and V. M. Vinokur, *Theor. Math. Phys.* **163**, 537 (2010).
 [28] L. Xu, S. V. Buldyrev, N. Giovambattista, C. A. Angell, and H. E. Stanley, *J. Chem. Phys.* **130**, 054505 (2009).
 [29] P. G. Wolynes and V. Lubchenko, *Structural Glasses and Supercooled Liquids: Theory, Experiment, and Applications* (Wiley, New Jersey, 2012).
 [30] H. Vogel, *Phys. Z.* **22**, 645 (1921); G. S. Fulcher, *J. Am. Ceram. Soc.* **8**, 339 (1925); G. Tammann and W. Hesse, *Z. Anorg. Allg. Chem.* **156**, 245 (1926).
 [31] It is known that T_g is somewhere between approximations of T_g obtained from (VF) and (MCT).
 [32] W. Götze, *J. Phys. C* **11**, A1 (1999); D. R. Reichman and P. Charbonneau, *J. Stat. Mech.* (2005) P05013.
 [33] R. Böhmer and C. A. Angell, *Phys. Rev. B* **45**, 10091 (1992).
 [34] C. De Michele, F. Sciortino, and A. Coniglio, *J. Phys. Condens. Matter* **16**, L489 (2004).
 [35] Z. Shi, P. G. Debenedetti, F. H. Stillinger, and P. Ginart, *J. Chem. Phys.* **135**, 084513 (2011).
 [36] S. Sengupta, F. Vasconcelos, F. Affouard, and S. Sastry, *J. Chem. Phys.* **135**, 194503 (2011).
 [37] C. A. Angell, K. L. Ngai, G. B. McKenna, P. F. McMillan, and S. W. Martin, *J. Appl. Phys.* **88**, 3113 (2000).